ChemPubSoc Europe

DOI: 10.1002/ejic.201800754

EurJIC European Journal of Inorganic Chemistry

Full Paper

Manganese Clusters | *Very Important Paper* |

VIP [Mn_{14}] "Structural Analogues" of Well-Known [Mn_{12}] Single-Molecule Magnets

Maria Charalambous,[a] Eleni E. Moushi,[a][‡] Tu N. Nguyen,[b] Andrew M. Mowson,[b] George Christou,[b] and Anastasios J. Tasiopoulos*[a]

Abstract: A new family of tetradecanuclear Mn clusters $[Mn^{III}_{10}Mn^{IV}_4(\mu_3\text{-}O)_{12}(EtCO_2)_{12}(pd)_4(EtOH)_4(py)_4](ClO_4)_2$ (**1**), $[Mn^{III}_{10}Mn^{IV}_4(\mu_3\text{-}O)_{12}(EtCO_2)_{12}(mpd)_4(EtOH)_2(H_2O)_2(py)_4](ClO_4)_2$ (**2**), and $[Mn^{III}_{10}Mn^{IV}_4(\mu_3\text{-}O)_{12}(MeCO_2)_{10}(pic)_4(pd)_4(pdH_2)_4]$ [**3**] (picH = picolinic acid) were prepared from the use of the aliphatic diols 1,3-propanediol (pdH_2) and 2-methyl-1,3-propanediol ($mpdH_2$). The $[Mn^{III}_{10}Mn^{IV}_4]$ aggregates consist of a $[Mn^{III}_{10}]$ outer ring surrounding a $[Mn^{IV}_4]$ defective dicubane. Interestingly, the core of **1**–**3** is similar to those of a $[Mn_{12}(\mu_3\text{-}O)_{12}(RCO_2)_{16}(H_2O)_4]$ "normal $[Mn_{12}]$" and a modified $[Mn_{12}]$ aggregate consisting of a $[Mn^{III}_8]$ ring, surrounding a $[Mn^{IV}_4]$ defective dicubane called "flat $[Mn_{12}]$". Dc and ac magnetic susceptibility studies revealed the presence of dominant antiferromagnetic exchange interactions in complexes **1**–**3** leading to small spin ground-state values.

Introduction

Mn carboxylate clusters continue to attract significant attention mainly because of their structural characteristics and physical properties.[1–9] In particular, Mn has three air-stable oxidation states, +2, +3, and +4 with an excellent affinity for ligands exhibiting a high bridging capability such as RCO_2^-, O^{2-}/OH^-, ROH/RO^-, and others. As a result, metal clusters can be formed with varying Mn oxidation states, bridging groups, and ligand coordination modes, etc. leading in turn to a remarkable structural diversity and a very fruitful and unique coordination chemistry. In addition, Mn clusters are also related to research fields that have attracted intense interest such as bioinorganic chemistry and molecular magnetism.[2–12] In the bioinorganic area, the interest in Mn cluster chemistry arises from the fact that a tetranuclear Mn cluster is located in the active site of photosystem II and is responsible for the photosynthetic oxidation of H_2O to molecular O_2.[10–12] However, the explosive interest in Mn carboxylate chemistry and molecular magnetism was triggered by the discovery that $[Mn_{12}(\mu_3\text{-}O)_{12}(MeCO_2)_{16}(H_2O)_4]$ ($[Mn_{12}Ac]$) exhibits superparamagnet-like slow magnetization relaxation and thus behaves as a nanoscale magnet at low temperatures.[8,13] Such compounds are termed single-molecule magnets (SMMs) to emphasize that their magnetic properties arise from the intrinsic intramolecular properties of individual molecules.[8]

This exciting discovery attracted the interest of scientists from diverse areas[8,9,14–19] and created the need for the synthesis of (i) more $[Mn_{12}(\mu_3\text{-}O)_{12}(RCO_2)_{16}(H_2O)_4]$ ($[Mn_{12}]$) derivatives and (ii) new structural types of Mn complexes to better study and understand physical phenomena related to single-molecule magnetism and also to obtain SMMs with enhanced properties. As a result various $[Mn_{12}]$ derivatives have been prepared in their neutral, one-, two- or three-electron reduced versions with a variety of carboxylate, mixed carboxylate, and mixed carboxylate/non-carboxylate ligands.[8,20–24] The synthesis of these compounds involved targeted structural modifications to preformed $[Mn_{12}]$ clusters.[8] In addition, in all such modifications, the $[Mn^{III}_8Mn^{IV}_4(\mu_3\text{-}O)_{12}]^{16+}$ (in the case of the neutral analogues) core consisting of a $[Mn^{III}_8(\mu_3\text{-}O)_8]^{8+}$ outer ring surrounding an inner $[Mn^{IV}_4(\mu_3\text{-}O)_4]^{8+}$ cube remains essentially the same.[8,20–25] However, there is a family of $[Mn_{12}]$ analogues in which the core is slightly changed. These $[Mn_{12}]$ complexes consist of a $[Mn^{III}_8(\mu_3\text{-}O)_8]^{8+}$ ring surrounding a flat $[Mn^{IV}_4(\mu_3\text{-}O)_2(\mu\text{-}MeO)_2(\mu\text{-}A)_2]^{n+}$ (A = O^{2-} or MeO^- or MeO^-/OH^-) defective dicubane.[26–28] In fact, their main difference from the "normal $[Mn_{12}]$" complexes is the presence of a flat $[Mn^{IV}_4]$ defective dicubane unit in the inner part of the core instead of a $[Mn^{IV}_4]$ cubane in the "normal $[Mn_{12}]$" cluster; for this reason this type of $[Mn_{12}]$ complex was termed "flat $[Mn_{12}]$".[26–28] Since the oxidation states of the metal ions of a "flat $[Mn_{12}]$" remain the same as in the "normal $[Mn_{12}]$" and the structural core is only slightly modified, this compound was also considered as a $[Mn_{12}]$ analogue with a slightly different core.[26–28] Notably, this compound was not isolated from controlled modification of the "normal $[Mn_{12}]$" as is the case for the synthesis of all other $[Mn_{12}]$ derivatives, but from a self-assembly synthetic method that involves reductive aggregation of MnO_4^- in methanol, in

[a] *Department of Chemistry, University of Cyprus, 1678 Nicosia, Cyprus*
E-mail: atasio@ucy.ac.cy
http://ucy.ac.cy/dir/en/component/comprofiler/userprofile/atasio
[b] *Department of Chemistry, University of Florida Gainesville, 32611-7200, USA*
[‡] Present address: Department of Life Sciences, School of Sciences, European University of Cyprus, 1516 Nicosia, Cyprus

Supporting information and ORCID(s) from the author(s) for this article are available on the WWW under https://doi.org/10.1002/ejic.201800754.

the presence of a carboxylic acid that provides carboxylate ligands and an acidic environment to avoid precipitation of Mn oxides/hydroxides.[26–28]

Interestingly, although [Mn_{12}] chemistry has been exhaustively investigated over the last 25 years, it still attracts significant interest.[15–17,21–25] In particular, there are still reports on the synthesis of new [Mn_{12}] derivatives[21] and also on the utilization of [Mn_{12}] analogues as building-blocks for the construction of oligomers[23] or multidimensional coordination polymers and as catalysts.[22,24] In addition, there is significant interest in the incorporation of [Mn_{12}] derivatives into the pores of metal organic frameworks and other types of porous materials.[25] Clearly intense synthetic efforts have been devoted to the synthesis and detailed investigation of the properties of [Mn_{12}] analogues and thus this family has been justifiably described as the Drosophila of SMMs, as it provides an invaluable source of comparative data on this fascinating magnetic phenomenon.[8]

Synthetic efforts targeting new structural types of Mn clusters have also been successful affording compounds with various shapes and nuclearities up to 84,[29] some of which exhibit SMM properties.[1–7,29–35] However, despite the structural diversity of Mn carboxylate chemistry and the intense synthetic efforts in this area there have been no structural analogues of the [Mn_{12}] SMMs reported in the literature that exhibit a slightly modified structural core except for the "flat [Mn_{12}]" compounds mentioned above.

We herein report on a new family of compounds [$Mn^{III}_{10}Mn^{IV}_4(\mu_3\text{-}O)_{12}(EtCO_2)_{12}(pd)_4(EtOH)_4(py)_4](ClO_4)_2$ (**1**), [$Mn^{III}_{10}Mn^{IV}_4(\mu_3\text{-}O)_{12}(EtCO_2)_{12}(mpd)_4(EtOH)_2(H_2O)_2(py)_4](ClO_4)_2$ (**2**), and [$Mn^{III}_{10}Mn^{IV}_4(\mu_3\text{-}O)_{12}(MeCO_2)_{10}(pic)_4(pd)_4(pdH_2)_4$] (**3**] (picH = picolinic acid, pdH_2 = 1,3-propanediol, $mpdH_2$ = 2-methyl-1,3-propanediol) consisting of a [$Mn^{III}_{10}(\mu_3\text{-}O)_8]^{14+}$ ring surrounding a [$Mn^{IV}_4(\mu_3\text{-}O)_4(\mu\text{-}RO)_2]^{6+}$ defective dicubane. The [$Mn^{III}_{10}Mn^{IV}_4(\mu_3\text{-}O)_{12}]^{22+}$ structural core of **1**–**3** displays a remarkable similarity to the cores of "flat [Mn_{12}]" and "normal [Mn_{12}]" clusters and is a unique example of a [Mn_{12}] structural analogue, despite its higher nuclearity. The syntheses, crystal structures, and magnetic properties of compounds **1**–**3** are reported.

Results and Discussion

Syntheses

We have been systematically investigating the use of diols in Mn carboxylate chemistry as a route to new high nuclearity clusters with novel structural features and interesting magnetic properties.[4a,31,32,36–38] These investigations have focused on the use of simple aliphatic diols such as pdH_2 and $mpdH_2$, which, because of their alkoxide arms, exhibit a high bridging capability and very rich coordination chemistry.[4a,31,36–38] Compounds **1**–**3** were prepared from reactions of [$Mn_3O(RCO_2)_6(py)_3]^{n+}$ [R = Et, n = 1, (**1**), (**2**); R = Me, n = 0, (**3**)] with pdH_2 (**1** and **3**) or $mpdH_2$ (**2**) in EtOH (**1** and **2**) or MeCN (**3**). The reaction mixture that led to the formation of **1** also contained $KMnO_4$, which likely acted as an oxidant. In fact reactions of Mn salts or preformed clusters in alcohols with MnO_4^- have afforded compounds exhibiting impressive crystal structures including the giant [Mn_{70}] and [Mn_{84}] wheels.[29,30] Similarly, the "flat [Mn_{12}]" complexes discussed above were prepared in MeOH from the reductive aggregation of MnO_4^- in the presence of a carboxylic acid.[26–28] Compound **1** was prepared from the investigation of reactions of preformed Mn clusters with pdH_2 in the presence of MnO_4^- in EtOH. Thus, the reaction of [$Mn_3O(EtCO_2)_6(py)_3](ClO_4)$ with pdH_2 in the presence of $KMnO_4$ in a molar ratio of about 2:20:1 in EtOH afforded compound **1**·$4H_2O$ in ca. 20 % yield based on total Mn content. The formation of compound **1** is summarized in Equation (1):

$$13\,[Mn_3O(EtCO_2)_6(py)_3](ClO_4) + 12\,pdH_2 + 3\,KMnO_4 + 12\,EtOH + 23\,H_2O \xrightarrow{EtOH} 3\,[Mn_{14}(\mu_3\text{-}O)_{12}(EtCO_2)_{12}(pd)_4(EtOH)_4(py)_4](ClO_4)_2{\cdot}4H_2O + 42\,EtCO_2H + 3\,KClO_4 + 4\,HClO_4 + 27\,py \quad (1)$$

After the isolation and crystallographic characterization of **1** was achieved, the synthesis of the analogous compound that would contain mpd^{2-} instead of pd^{2-} was targeted with priority. Complex **2** was isolated from a similar synthetic procedure to the one that afforded **1** which, however, did not involve the use of MnO_4^- in the reaction mixture. We believe that the oxidation of the Mn ions in this reaction (the average oxidation state of Mn ions in the Mn precursor compound and in **2** is 3 and 3.29, respectively) took place from atmospheric O_2. Thus, the reaction of [$Mn_3O(EtCO_2)_6(py)_3](ClO_4)$ with $mpdH_2$ in a molar ratio of about 1:10 in EtOH afforded compound **2**·$4H_2O$ in ca. 25 % yield based on total Mn content. The formation of compound **2**·$4H_2O$ is summarized in Equation (2):

$$14\,[Mn_3O(EtCO_2)_6(py)_3](ClO_4) + 12\,H_2mpd + 6\,EtOH + 34\,H_2O + 3\,O_2 \xrightarrow{EtOH} 3\,[Mn_{14}(\mu_3\text{-}O)_{12}(EtCO_2)_{12}(mpd)_4(EtOH)_2(H_2O)_2(py)_4](ClO_4)_2{\cdot}4H_2O + 48\,EtCO_2H + 8\,HClO_4 + 30\,py \quad (2)$$

After the isolation of **1** and **2** we focused on the synthesis of other analogues to extend this family of [Mn_{14}] clusters. In addition, we were interested in slightly modifying its structural characteristics aiming for analogues with improved magnetic properties. As a result various reactions of [$Mn_3O(RCO_2)_6(py)_3]^{n+}$ (n = 0 or 1) with pdH_2 or $mpdH_2$ under various reaction conditions were investigated. The modifications in the procedures that led to **1** and **2** included among others the employment of additional chelating ligands and the use of different reaction solvents. In particular, the reaction of [$Mn_3O(MeCO_2)_6(py)_3$]·py with pdH_2 and picH in a molar ratio of about 1:20:3 in EtOH afforded compound **3**·$4H_2O$ in ca. 25 % yield based on total Mn content. The formation of compound **3** is summarized in Equation (3):

$$14\,[Mn_3O(MeCO_2)_6(py)_3]{\cdot}py + 24\,pdH_2 + 12\,picH + 9\,H_2O + 6.5\,O_2 \xrightarrow{MeCN} 3\,[Mn_{14}(\mu_3\text{-}O)_{12}(MeCO_2)_{10}(pic)_4(pd)_4(pdH_2)_4] + 54\,MeCO_2H + 56\,py \quad (3)$$

Description of the Structures

Complexes **1**, **2**, and **3**·2MeCN crystallize in the triclinic space group $P\bar{1}$ with the asymmetric units of **1** and **2** containing half the $[Mn_{14}]^{2+}$ cationic cluster and one $[ClO_4]^-$ counter anion and

that of **3** containing half the neutral [Mn_{14}] cluster and one MeCN solvent molecule of crystallization. The three [Mn_{14}] clusters exhibit related structural cores with their main differences appearing in their peripheral ligation. Thus, the structure of **1** shall be discussed in detail and compared to the structures of **2** and **3**. The molecular structure and the structural core of **1** are shown in Figure 1 and selected bond lengths and angles are summarized in Table S1 in the Supporting Information. Selected bond lengths and angles for **2** and **3** and representations of the molecular structure of **2** and structural core of **2** and **3** are shown in Tables S2 and S3 and Figures S1 and S2, respectively in the Supporting Information. A representation of the molecular structure of **3** is shown in Figure 2.

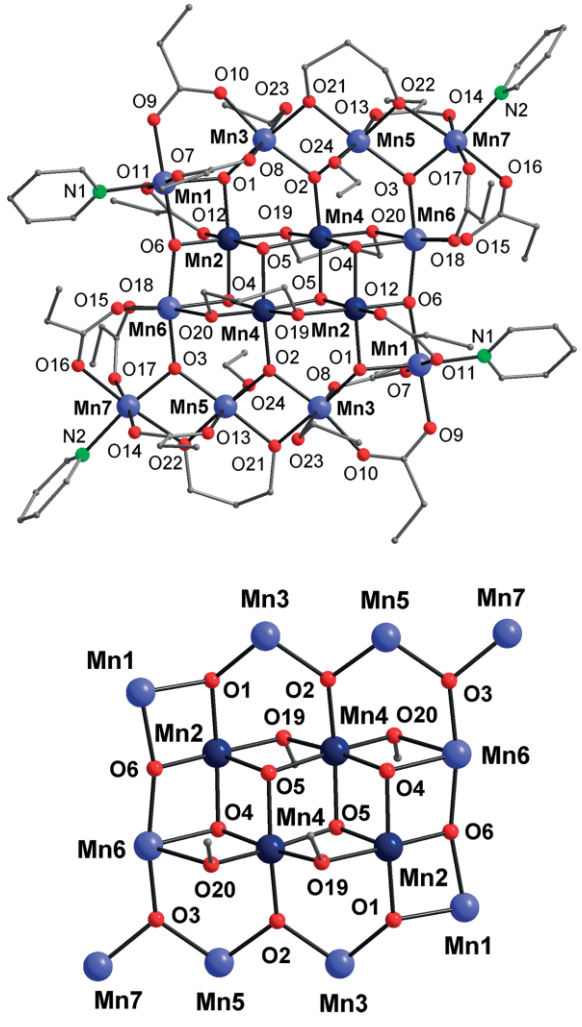

Figure 1. Labeled representations of the molecular structure of compound **1** (top) and its structural core (bottom). Color code: Mn^{III} light blue; Mn^{IV} dark blue; O red; N green, C grey. H atoms are omitted and symmetry relations are not indicated for clarity.

The [$Mn^{III}_{10}Mn^{IV}_4$] cation consists of a [Mn^{III}_{10}] outer ring surrounding a [Mn^{IV}_4] defective dicubane. The Mn^{IV} ions of the latter are linked together through four μ_3-O^{2-} anions and two alkoxide μ-RO^- arms of two pd^{2-} ligands bridging in a $\eta^2{:}\eta^2{:}\mu_3$ coordination mode resulting in the formation of a face-sharing dicubane subunit with two missing vertices. Two of the μ_3-O^{2-} anions bridge exclusively Mn^{IV} ions of the central [Mn^{IV}_4] subunit and the other two bridge one Mn^{III} and two Mn^{IV} ions, thus linking the [Mn^{IV}_4] defective dicubane to the outer [Mn^{III}_{10}] ring. The two subunits are also connected through two alkoxide μ-RO^- arms of two pd^{2-} ligands mentioned above, two $\eta^1{:}\eta^1{:}\mu$-$EtCO_2^-$ ligands, and 6 μ_3-O^{2-} anions bridging one Mn^{IV} and two Mn^{III} ions with the Mn ions of the inner unit linked either to one or to two such μ_3-O^{2-} ions. These six μ_3-O^{2-} and two additional μ_3-O^{2-} ligands bridging exclusively Mn^{III} ions connect the ten Mn^{III} ions of the outer ring forming the [$Mn^{III}_{10}(\mu_3\text{-}O)_8$]$^{14+}$ structural core. This ring is similar to the [Mn^{III}_8] outer ring appearing in known [Mn_{12}] complexes,[8,20–24,26–28] where the most obvious difference between them is the presence of two additional Mn^{III} ions each of which is connected through a μ_3-O^{2-} ion to two Mn^{III} ions forming a [$Mn^{III}_3(\mu_3\text{-}O)$]$^{7+}$ triangle. Two $\eta^1{:}\eta^1{:}\mu$-$EtCO_2^-$ ligands and one $\eta^1{:}\eta^1{:}\mu$-$EtCO_2^-$/one alkoxide μ-RO^- arm of a $\eta^2{:}\eta^2{:}\mu_3$ pd^{2-} ligand bridge two of the edges of the triangle. Each triangle is linked through the second μ-RO^- group of the above mentioned pd^{2-} and one O^{2-} on one side and an O^{2-} ligand on the other side to two [$Mn^{III}_2O(EtCO_2)_2$]$^{2+}$ moieties forming the [Mn^{III}_{10}] outer ring. The peripheral ligation of complex **1** is completed by terminal solvent molecules and in particular four py and four EtOH molecules ligated to Mn^{III} ions. All propionate ligands bridge in their common *syn, syn*-$\eta^1{:}\eta^1{:}\mu$ mode whereas the four pd^{2-} anions bridge in a $\eta^2{:}\eta^2{:}\mu_3$ coordination mode. All Mn ions are hexacoordinate adopting a distorted octahedral coordination geometry with the Mn^{III} ones displaying the expected Jahn–Teller (JT) elongations. However, the JT axes are not coparallel since those of the two Mn^{III} ions that are not bridged to the inner [Mn^{IV}_4] subunit are not coparallel to the other eight (see Figure S3 in the Supporting Information). The oxidation states of the Mn ions and the protonation levels of the ligands were determined by bond valence sum calculations, charge considerations, and inspection of metric parameters.[39,40] The Mn^{III}–O or Mn^{III}–N bond lengths range from 1.839(3) to 2.288(4) Å whereas the Mn^{IV}–O ones from 1.833(4) to 1.938(4) and are in agreement with the literature values. The neighboring [Mn_{14}] clusters are fairly well separated with the shortest Mn···Mn distance (ca. 7.98 Å) appearing between two Mn1 ions. The fairly short distance between Mn1 ions of neighboring units of **1** may be attributed to the existence of π–π stacking interactions between the py rings (average intermolecular C···C distance is about 3.5 Å) ligated to Mn1 of different molecules.

The structure of complex **2** is related to that of **1** with the main differences being (i) the presence of mpd^{2-} ligands instead of pd^{2-} and (ii) different terminal solvent molecules completing the peripheral ligation (4 EtOH/4 py in **1** vs. 2EtOH/2H_2O/4 py in **2**). Compound **3**, (Figure 2) on the other hand, although it contains the [$Mn^{III}_{10}Mn^{IV}_4(\mu_3\text{-}O)_{12}$]$^{22+}$ structural core that is also present in **1** and **2**, exhibits structural features that are not shown in these two compounds. These arise from the presence of four picolinate molecules in the structure of **3**; each one is linked through the pyridine N atom and the carboxylate O to a Mn ion (Mn1 and Mn7 are linked to pic^- ligands), thus forming a five-membered chelating ring. The insertion of four chelating ligands in the [Mn_{14}] cluster resulted in several modifications in the peripheral ligation. In particular, compound **3**

contains only four terminal neutral pdH$_2$ ligands in contrast to **2** and **3**, which contain eight terminally ligated solvent molecules. In addition, compound **3** contains less and also different types of carboxylate ligands (ten $MeCO_2^-$) compared with **1** and **2** (that contain twelve $EtCO_2^-$ ligands). In particular, one of the two carboxylate ions bridging in one edge of the triangles of the $[Mn^{III}_{10}]$ ring in **1** and **2** do not appear in **3**; thus this edge in **3** is bridged only from one acetate ligand. Furthermore, in **3**, as also happens in **1** and **2**, the inner $[Mn^{IV}_4]$ defective dicubane is linked to the outer $[Mn^{III}_{10}]$ ring through two carboxylate ligands; however, the inner $[Mn^{IV}_4]$ subunit in **3** is bridged through a carboxylate group to a Mn^{III} ion located in the $[Mn^{III}_3O]^{7+}$ triangle whereas in **1** and **2** it is bridged to a Mn^{III} ion of a dinuclear $[Mn^{III}_2]$ moiety of the outer $[Mn^{III}_{10}]$ ring. Another difference in the structure of **3** compared to those of **1** and **2** is in the orientation of the JT axes of the octahedral Mn^{III} ions. In particular, in **3**, as also observed in **1** and **2**, eight of these axes are coparallel; however, in **3** the JT axes that are not coparallel to the other eight appear in the dinuclear $[Mn^{III}_2]$ moiety, whereas in **1** and **2** they are located in the $[Mn^{III}_3O]^{7+}$ triangle (Figure S3).

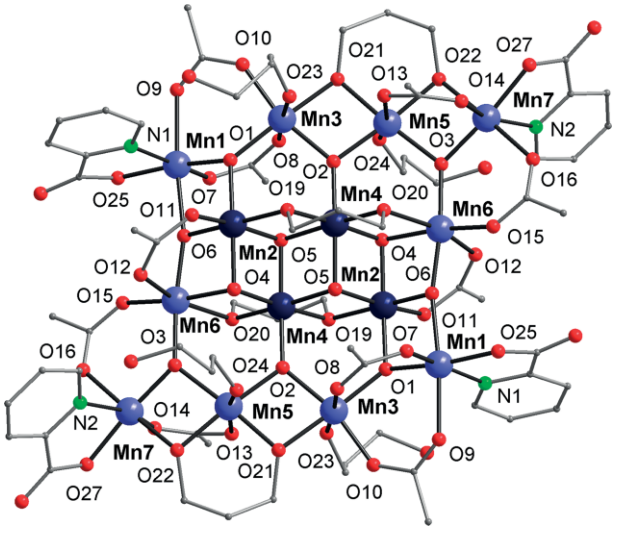

Figure 2. Labeled representation of the molecular structure of compound **3**. Color code: Mn^{III} light blue; Mn^{IV} dark blue; O red; N green, C grey. H atoms are omitted and symmetry relations are not indicated for clarity.

Clearly the formation of complex **3** that contains the same Mn/O core with **1** and **2** and an additional chelating ligand (pic^-) completing its peripheral ligation reveals the significant stability of the $[Mn^{III}_{10}Mn^{IV}_4(\mu_3\text{-}O)_{12}]^{22+}$ core. As discussed above, the presence of pic^- resulted in several structural modifications confirming the versatility of this core and its capability to be formed with various ligands. The isolation of **3** thus suggests that this core can also be stabilized with other chelating ligands or with a combination of chelating ligands.

Interestingly, the $[Mn^{III}_{10}Mn^{IV}_4(\mu_3\text{-}O)_{12}]^{22+}$ core is similar to the structural cores of the "flat $[Mn_{12}]$" and "normal $[Mn_{12}]$" complexes (Figure 3). The core of "normal $[Mn_{12}]$" complexes consisting of an outer $[Mn^{III}_8(\mu_3\text{-}O)_8]^{8+}$ ring surrounding a central $[Mn^{IV}_4(\mu_3\text{-}O)_4]^{8+}$ cube has been shown to be quite solid since it is not affected from the significant variations in its peripheral ligation in the over 50 analogues reported to date.[8,20–24] On the other hand the core of "flat $[Mn_{12}]$" complexes consisting of a $[Mn^{III}_8(\mu_3\text{-}O)_8]^{8+}$ ring surrounding a $[Mn^{IV}_4]$ defective dicubane has been observed only in three examples, namely $(NBu^n_4)_2[Mn^{III}_8Mn^{IV}_4O_{12}(MeO)_2(PhCO_2)_{16}(H_2O)_2]$ (**4**),[26,27] $[Mn^{III}_8Mn^{IV}_4O_{10}(MeO)_3(OH)(C_6H_3F_2CO_2)_{16}(MeOH)_2]$ (**5**),[28] and $[Mn^{III}_8Mn^{IV}_4O_{10}(MeO)_4(Bu^tCO_2)_{16}(MeOH)_2]$ (**6**).[28] This core displays some structural flexibility since the inner Mn^{IV} ions apart from two $\mu_3\text{-}O^{2-}$ are also bridged by two $\mu\text{-}O^{2-}$/2μ-MeO^- (**4**) or three μ-MeO^-/one μ-OH^- (**5**), or four μ-MeO^- (**6**) ligands. The structural core of **1**–**3** exhibits a remarkable similarity to those of **4**–**6** (Figure 3), especially if one takes into consideration their different nuclearities. In fact, the major difference between these two structural cores is the presence of two additional Mn^{III} ions in the outer ring of the $[Mn^{III}_{10}Mn^{IV}_4(\mu_3\text{-}O)_{12}]^{22+}$ core of **1**–**3**. There are also other differences between the two cores in the way that the outer $[Mn^{III}_{10}]$ ring is linked to the inner $[Mn^{IV}_4]$ defective dicubane. In particular, in the case of **1**–**3**, two of the inner Mn^{IV} ions are linked to one $\mu_3\text{-}O^{2-}$ and two to two $\mu_3\text{-}O^{2-}$ ions of the outer $[Mn^{III}_{10}(\mu_3\text{-}O)_8]^{14+}$ ring whereas in **4**–**6** all Mn^{IV} ions are linked to two O^{2-} ions of the

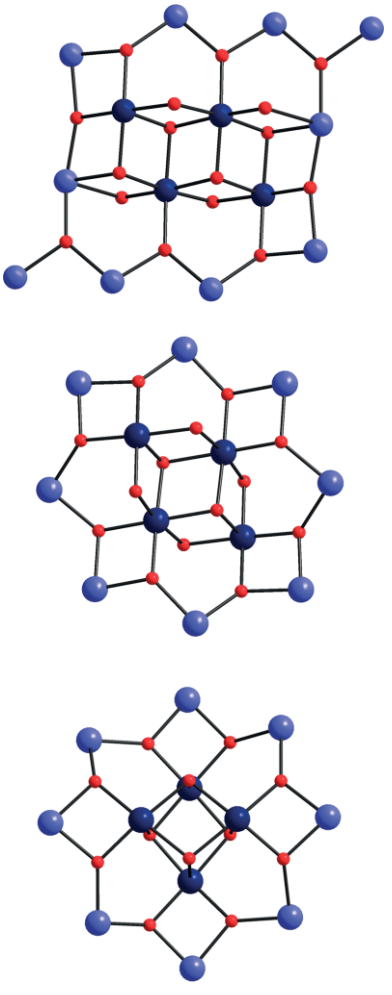

Figure 3. Comparison of the $[Mn^{III}_{10}Mn^{IV}_4(\mu_3\text{-}O)_{12}]^{22+}$ structural core of **1**–**3** (top), the $[Mn^{III}_8Mn^{IV}_4(\mu_3\text{-}O)_{10}(\mu\text{-}O)_2(\mu\text{-}MeO)_2]^{14+}$ of a "flat $[Mn_{12}]$" (compound **4**) (middle), and the $[Mn^{III}_8Mn^{IV}_4(\mu_3\text{-}O)_{12}]^{16+}$ of a "normal $[Mn_{12}]$" cluster. Color code: Mn^{IV} dark blue; Mn^{III} light blue; O red.

outer ring. In addition, in **4**–**6** the monoatomic bridges building the inner $[Mn^{IV}_4(\mu_3\text{-}O)_2(\mu\text{-}MeO)_2(\mu\text{-}A)_2]^{n+}$ (A = O^{2-} or MeO^- or MeO^-/OH^-) defective dicubane core are not connected to the Mn ions of the outer ring whereas in **1**–**3** two of the monoatomic $\mu_3\text{-}O^{2-}$ bridges connect two Mn^{IV} ions of the $[Mn^{IV}_4]$ moiety and one Mn^{III} ion of the outer $[Mn^{III}_{10}]$ ring. In any case, despite these structural differences the structural cores of **1**–**3** and **4**–**6** are related. In addition, the core of **1**–**3** displays similarities to that of "normal $[Mn_{12}]$" complexes as shown in Figure 3. Clearly, although there are other compounds reported based on an outer $[Mn^{III}_x]$ subunit surrounding an inner $[Mn^{IV}_y]$ moiety including various $[Mn_{16}]$[41] and $[Mn_{21}]$[42] aggregates, complexes **1**–**3** are the closest related analogues of the "normal" and "flat" $[Mn_{12}]$ SMMs.

Magnetic Properties

Solid-state dc magnetic susceptibility measurements were performed on polycrystalline samples of complexes **1**·$4H_2O$, **2**·$4H_2O$, and **3**, under a magnetic field of 0.1 T in the temperature range 5–300 K. The obtained data are shown as $\chi_M T$ vs. T plots in Figure 4. For complex **1**·$4H_2O$ and **2**·$4H_2O$ the $\chi_M T$ value decreases steadily from 24.54 and 25.23 $cm^3\ mol^{-1}\ K$ at 300 K to 1.75 and 1.86 $cm^3\ mol^{-1}\ K$ at 5 K, respectively. For **3**, the $\chi_M T$ value at 300 K is 21.76 $cm^3\ mol^{-1}\ K$ and decreases smoothly with decreasing temperature reaching a value of about 15 $cm^3\ mol^{-1}\ K$ at 70 K and then rapidly decreases to 4.51 $cm^3\ mol^{-1}\ K$ at 5.0 K (Figure 4). In all compounds the 300 K $\chi_M T$ value is significantly lower than the corresponding spin-only (g = 2) value of 37.5 $cm^3\ mol^{-1}\ K$ expected for compounds consisting of 10 Mn^{III}/4 Mn^{IV} non-interacting ions indicating the presence of dominant antiferromagnetic interactions. The overall profiles of the $\chi_M T$ vs. T plots indicate a similar magnetic behavior for **1**·$4H_2O$ and **2**·$4H_2O$, since the two curves are nearly superimposed showing a significant decrease of $\chi_M T$ values even at high temperatures indicative of the presence of strong antiferromagnetic interactions. In the case of complex **3**, the overall magnetic behavior is slightly different as there is a rather smooth decrease of $\chi_M T$ up to 70 K suggesting the existence of weaker antiferromagnetic interactions. The 5 K $\chi_M T$ values indicate very small, or diamagnetic spin ground-state values for all compounds although the $\chi_M T$ value for **3** is higher than the corresponding ones for **1**·$4H_2O$ and **2**·$4H_2O$ suggesting that the three complexes may have different S_T values.

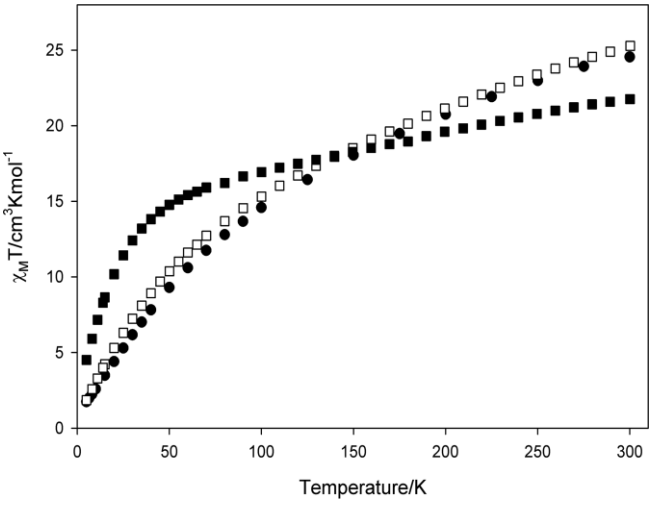

Figure 4. $\chi_M T$ vs. T plots for complexes **1** (●), **2** (□), and **3** (■) over the temperature range 5–300 K in a 0.1 T applied dc field.

Given the size of the $[Mn_{14}]$ cluster of **1**·$4H_2O$–**3** and the resulting number of inequivalent exchange constants, it was not possible to apply the Kambe method to determine the individual pairwise Mn_2 exchange interaction parameters. We concentrated instead on obtaining additional information on the ground-state spin, S_T, from ac magnetic susceptibility studies in a zero dc field and a 3.5 G ac field. Ac susceptibility studies are a powerful complement to dc studies for determining the ground state of a system, because they remove the complications arising from the presence of a dc field. The obtained in-phase χ'_M and out-of-phase χ''_M signals for complexes **1**·$4H_2O$–**3** are plotted as $\chi'_M T$ vs. T and χ''_M vs. T in Figures S4–S9 in the Supporting Information. The $\chi'_M T$ value for **1**·$4H_2O$–**3** decreases steadily with decreasing temperature from 15 to 1.8 K. Extrapolation of the $\chi'_M T$ data from $T \approx 4$ K to 0 K, at which point only the ground state will be populated, gives values of ca. 1, ca. 0.8, and ca. 2.5 $cm^3\ mol^{-1}\ K$ for **1**·$4H_2O$, **2**·$4H_2O$, and **3**, respectively. The observed values are consistent with spin ground-state values S_T = 1 for **1**·$4H_2O$ and **2**·$4H_2O$ and S_T = 2 for **3**. These studies indicate a spin variability in **1**·$4H_2O$–**3**, which although they have analogous structures, they exhibit different magnetic behavior. This spin variability has also been observed in the family of "flat Mn_{12}" clusters that have related cores with **1**·$4H_2O$–**3** (vide supra). In particular, the three known compounds **4**, **5**, and **6** display S_T values of 6,[26,27] 5,[28] and 9,[28] respectively, with compounds **4** and **6** exhibiting SMM behavior as well. Interestingly, the S_T = 1 (**1**, **2**) and S_T = 2 (**3**) values can be rationalized assuming the presence of two additional Mn^{III} ions in **5** and **4**, respectively interacting antiferromagnetically with the $[Mn_{12}]$ complexes. Finally, complex **1**·$4H_2O$ exhibits a very weak out-of-phase ac signal at very low T whereas complexes **2**·$4H_2O$ and **3** do not exhibit any out-of-phase ac signals down to 1.8 K. Thus, we conclude that **1**·$4H_2O$ might be a very weak SMM whereas **2**·$4H_2O$ and **3** do not exhibit SMM behavior.

Conclusions

Summarizing, three new compounds **1**–**3** have been prepared from the use of the aliphatic diols pdH_2 and $mpdH_2$ in Mn cluster chemistry. They exhibit a $[Mn^{III}_{10}Mn^{IV}_4(\mu_3\text{-}O)_{12}]^{22+}$ structural core that is related to the Mn/O^{2-} cores of "flat $[Mn_{12}]$" and "normal $[Mn_{12}]$" clusters. Especially the $[Mn^{III}_8Mn^{IV}_4(\mu_3\text{-}O)_{10}(\mu\text{-}MeO)_2(\mu\text{-}A)_2]^{n+}$ (A = O^{2-} or MeO^- or MeO^-/OH^-) core of "flat $[Mn_{12}]$" exhibits a remarkable similarity to the $[Mn^{III}_{10}Mn^{IV}_4(\mu_3\text{-}O)_{12}]^{22+}$ one of **1**–**3** with their main difference being the presence of two additional Mn ions in the $[Mn_{14}]$ complexes. This reveals the versatility of this core, which can be stabilized with various modifications. Notably complexes **1**–**3** exhibit differences in their peripheral ligation. These are rather small for complexes **1** and **2** but quite significant for **1** (or **2**) and **3**. The significantly different peripheral ligation of compounds **1** or **2**

and **3**, despite the fact that they have a nearly identical structural core, is attributed to the presence in the structure of **3** of pic^-, i.e. an additional chelating ligand. Magnetism studies indicated the existence of dominant antiferromagnetic interactions in **1**–**3**, which lead to small or possibly diamagnetic spin ground states. Notably the magnetic behavior of **1** and **2** is very similar to each other and different from the overall magnetic behavior of **3**. The isolation of **1**–**3** emphasizes the versatility of the structural cores of well-known $[Mn_{12}]$ SMMs. In addition, the capability of the core of **1**–**3** to be stabilized in the presence of additional chelating ligands as confirmed from the isolation of **3** indicates that it is amenable to several modifications. Investigations targeting new analogues with significantly different peripheral ligation are in progress targeting $[Mn_{14}]$ derivatives that may exhibit interesting magnetic properties.

Experimental Section

Materials and Physical Measurements

All manipulations were performed under aerobic conditions using chemicals and solvents as received, unless otherwise stated. $[Mn_3O(MeCO_2)_6(py)_3]$·py and $[Mn_3O(EtCO_2)_6(py)_3](ClO_4)$ were prepared as described previously.[43]

IR spectra were recorded in the solid state (KBr pellets) in the 4000–400 cm^{-1} range using a Shimadzu Prestige-21 spectrometer. Elemental analysis (C, H, and N) were performed by the in-house facilities of the Chemistry Department at the University of Florida.

Variable-temperature dc magnetic susceptibility data down to 1.8 K were collected with a Quantum Design MPMS-XL SQUID magnetometer equipped with a 70 kG (7 T) dc magnet at the University of Florida. Diamagnetic corrections were applied to the observed paramagnetic susceptibilities using Pascal's constants. Samples were embedded in solid eicosane to prevent torquing in the dc field. Ac magnetic susceptibility data were collected on the same instrument employing a 3.5 G ac field oscillating at frequencies up to 1500 Hz.

$[Mn_{14}(\mu_3\text{-}O)_{12}(EtCO_2)_{12}(pd)_4(EtOH)_4(py)_4](ClO_4)_2$ (1): PdH_2 (200 µL, 2.8 mmol) and solid $KMnO_4$ (0.02 g, 0.13 mmol) were added to a stirred brown solution of $[Mn_3O(EtCO_2)_6(py)_3](ClO_4)$(0.26 g, 0.27 mmol) in EtOH (12 mL) and the reaction mixture was left under magnetic stirring for about1 h. The resulting brown slurry was filtered and the brown filtrate was divided into small portions (3 mL each), which were placed in glass vials and layered with Et_2O (3:1 v/v). The vials were sealed with a stopper and left undisturbed at room temperature. After one week, brown crystals of **1** appeared suitable for X-ray structural determination. The crystals were isolated by filtration, washed with EtOH and dried in vacuo; the yield was ca. 20 %. The crystals for X-ray studies were kept in contact with the mother liquor to prevent solvent loss. $C_{76}H_{136}N_4O_{60}Cl_2Mn_{14}$ (**1**·$4H_2O$): calcd. C 31.41, H 4.72, N 1.93; found C 31.05, H 4.45, N 1.73. Selected IR data (KBr pellet): $\tilde{\nu}$ = 3123 (s, br), 2773 (w), 1697 (m), 1576 (m), 1394 (s), 1064 (m) 613 (m, br) cm^{-1}.

$[Mn_{14}(\mu_3\text{-}O)_{12}(EtCO_2)_{12}(mpd)_4(EtOH)_2(H_2O)_2(py)_4](ClO_4)_2$ (2): $MpdH_2$ (200 µL, 2.25 mmol) was added to a stirred solution of $[Mn_3O(EtCO_2)_6(py)_3](ClO_4)$ (0.22 g, 0.225 mmol) in EtOH (8 mL). The resulting brown solution was left under magnetic stirring for about 2.5 hours leading to a red-brown slurry. The slurry was filtered and the brown filtrate was divided into small portions (3 mL each), which were placed in glass vials and layered with Et_2O (3:1 v/v). The vials were sealed with stoppers and left undisturbed at room temperature. After two weeks, brown crystals of **2**·$4H_2O$ were formed, suitable for X-ray structural determination. The crystals were isolated by filtration, washed with EtOH, and dried in vacuo; the yield was ca. 25 %. The crystals for X-ray studies were kept in contact with the mother liquor to prevent solvent loss. $C_{76}H_{136}N_4O_{60}Cl_2Mn_{14}$ (**2**·$4H_2O$): calcd. C 31.41, H 4.72, N 1.93; found C 31.35, H 4.42, N 1.86. Selected IR data (KBr pellet): $\tilde{\nu}$ = 3445 (s, br), 2978 (w), 2940 (w), 1584 (m), 1544 (w), 1385 (m), 1091 (m), 625 (m, br) cm^{-1}.

$[Mn_{14}(\mu_3\text{-}O)_{12}(MeCO_2)_{10}(pic)_4(pd)_4(pdH_2)_4]$ (3): PdH_2 (0.40 mL, 5.534 mmol) and picolinic acid (0.10 g, 0.812 mmol) were added to a stirred solution of $[Mn_3O(MeCO_2)_6(py)_3]$·py (0.24 g, 0.277 mmol) in MeCN (12 mL). The reaction mixture was left under magnetic stirring for about 2 h, then the resulting brown slurry was filtered and the brown filtrate was left undisturbed at room temperature. Dark brown crystals of **3**·2MeCN suitable for X-ray structural determination appeared after a few weeks, isolated by filtration, washed with MeCN and dried in vacuo; the yield was ca. 25 %. The crystals for X-ray studies were kept in contact with the mother liquor to prevent solvent loss. The dried sample was analyzed satisfactorily as solvent-free **3**. $C_{68}H_{102}O_{56}N_4Mn_{14}$ (**3**): calcd. C 30.93, H 3.89, N 2.12; found C 30.55, H 3.70, N 1.85. Selected IR data (KBr pellet): $\tilde{\nu}$ = 3420(s, br), 2948 (w), 2841 (w), 1669 (m), 1569 (s), 1412 (s), 1336 (s), 1292 (w), 1164 (m), 1057 (m), 939 (w), 709 (m), 617 (s), 520 (w) cm^{-1}.

Single Crystal X-ray Crystallography: Single crystal X-ray diffraction data for **1**, **2**, and **3**·2MeCN were collected with an Oxford-Diffraction Supernova diffractometer, equipped with a CCD detector utilizing Mo-K_α (λ = 0.71073 Å) for **1** and **3**·2MeCN and Cu-K_α (λ = 1.5418 Å) radiation for **2**. A suitable crystal was mounted on a Hampton cryoloop with Paratone-N oil and transferred to a goniostat where it was cooled for data collection. Empirical absorption corrections (multiscan based on symmetry-related measurements) were applied using CrysAlis RED software.[44] The structures were solved by direct methods using SIR2004[45] and refined on F^2 using full-matrix least-squares with SHELXL-2014/7[46] The software packages used were as follows: CrysAlis CCD for data collection,[44] CrysAlis RED for cell refinement and data reduction,[44] WINGX for geometric calculations,[47] and DIAMOND[48] for molecular graphics. The non-H atoms were treated anisotropically, whereas the aromatic H atoms were placed in calculated, ideal positions and refined as riding on their respective carbon atoms. However, there were a few H atoms in each crystal structure that we were neither able to locate nor model. These include (a) the H atoms attached to the ligated O atom of EtOH molecules for compound **1** (in total four H atoms were not located), (b) the $-CH_2-$ H atoms of four $EtCO_2^-$ ligands, the R_3CH group H atoms of the mpd^{2-} ligands, the H atoms of the ligated H_2O molecules, and the H attached to the ligated O atom of the EtOH molecules for compound **2** (in total 18 H atoms were not located), and (c) the H atoms linked to the coordinated O atom of the terminal pdH_2 molecules for **3**·2MeCN (in total four H atoms). Several restraints (DFIX, ISOR, DELU) have been applied in order to limit the disorder of the $EtCO_2^-$ ligands (for **1** and **2**), $MeCO_2^-$ ligands (for **3**), pd^{2-} (for **1** and **3**·2MeCN), mpd^{2-} (for **2**), pdH_2 (for **3**·2MeCN), and MeCN lattice solvent molecules (for **3**·2MeCN). Electron density contributions from disordered guest molecules were handled using the SQUEEZE procedure from the PLATON software suit.[49] Selected crystal data for **1**, **2**, and **3**·2MeCN are summarized in Table 1.

CCDC 1846492 (for **[1]**), 1846499 (for **[2]**), and 1846490 (for **[3]**·2MeCN) contain the supplementary crystallographic data for

Table 1. Crystallographic data for complexes **1**, **2**, and **3**·2MeCN.

	1	**2**	**3**·2MeCN
Empirical formula	$Mn_{14}Cl_2O_{56}N_4C_{76}H_{124}$	$Mn_{14}Cl_2O_{56}N_4C_{76}H_{110}$	$Mn_{14}O_{56}N_6C_{72}H_{104}$
M_r [g mol^{-1}]	2829.84	2815.75	2718.78
Space group	$P\bar{1}$	$P\bar{1}$	$P\bar{1}$
α [Å]	11.1602(9)	13.949(2)	12.039(2)
b [Å]	17.118(2)	14.430(2)	14.8320(9)
c [Å]	17.666(2)	15.067(2)	16.8936(9)
α [°]	72.122(5)	84.375(7)	67.356(5)
β [°]	81.587(6)	71.028(7)	77.653(6)
γ [°]	79.044(6)	73.634(7)	71.640(6)
V [Å^3]	3139.4(4)	2751.6(4)	2627.4(3)
Z	1	1	1
T [K]	100(2)	100(2)	100(2)
Radiation (λ)	Mo-K_α (0.71073)	Cu-K_α (1.54184)	Mo-K_α (0.71073)
$\rho_{calcd.}$ [g cm^{-3}]	1.497	1.699	1.718
μ [mm^{-1}]	1.481	13.865	1.717
Measured/independent reflections (R_{int})	23137/11048 (0.0542)	19509/9790 (0.0567)	19116/9229 (0.0691)
Observed reflections[a]	6656	6925	5630
R_1 [%][a,b]	7.31	7.67	8.76
wR_2 [%][c,d]	22.13	23.29	27.35

[a] $I > 2\sigma(I)$. [b] $R_1 = 100\Sigma(||F_o| - |F_c||) / \Sigma|F_o|$. [c] All data. [d] $wR_2 = 100\{\Sigma[w(F_o^2 - F_c^2)^2] / \Sigma[w(F_o^2)^2]^{1/2}\}$, $w = 1 / \sigma^2(F_o^2) + [(ap)^2 + bP]$, where $P = [\max(F_o^2,0) + 2F_c^2] / 3$.

this paper. These data can be obtained free of charge from The Cambridge Crystallographic Data Centre.

Supporting Information (see footnote on the first page of this article): Selected bond lengths and angles for **1**, **2**, and **3** and representations of the molecular structure of **2** and structural core of **2** and **3**, orientation of the JT axes of the octahedral Mn^{III} ions in **1**, **2**, and **3**, and the obtained in-phase χ'_M and out-of-phase χ''_M ac signals for complexes **1**·4H_2O, **2**·4H_2O and **3** plotted as χ'_MT vs. T and χ''_M vs. T.

Acknowledgments

This work was supported by the Cyprus Research Promotion Foundation Grant "PENEK/0311/04"', which is co-funded by the Republic of Cyprus and the European Regional Development Fund. GC thanks the National Science Foundation (NSF) for support (CHE-1565664). We also thank the European Union Seventh Framework Program (FP7/2007-2013) under Grant agreement number PIRSES-GA-2011-295190.

Keywords: Manganese · Polynuclear complexes · Polyols · X-ray diffraction · Magnetic properties · Cluster compounds

[1] G. E. Kostakis, A. M. Ako, A. K. Powell, *Chem. Soc. Rev.* **2010**, *39*, 2238–2271.
[2] C. Papatriantafyllopoulou, E. E. Moushi, G. Christou, A. J. Tasiopoulos, *Chem. Soc. Rev.* **2016**, *45*, 1597–1628.
[3] J. Ferrando-Soria, J. Vallejo, M. Castellano, J. Martínez-Lillo, E. Pardo, J. Cano, I. Castro, F. Lloret, R. Ruiz-García, M. Julve, *Coord. Chem. Rev.* **2017**, *339*, 17–103.
[4] a) A. J. Tasiopoulos, S. P. Perlepes, *Dalton Trans.* **2008**, 5537–5555; b) E. K. Brechin, *Chem. Commun.* **2005**, 5141–5153.
[5] a) A. Escuer, J. Esteban, S. P. Perlepes, T. C. Stamatatos, *Coord. Chem. Rev.* **2014**, *275*, 87–129; b) Y.-Z. Zheng, G.-J. Zhou, Z. Zheng, R. E. P. Winpenny, *Chem. Soc. Rev.* **2014**, *43*, 1462–1475; c) M. Nakano, H. Oshio, *Chem. Soc. Rev.* **2011**, *40*, 3239–3248; d) G. Aromı, D. Aguila, P. Gamez, F. Luis, O. Roubeau, *Chem. Soc. Rev.* **2012**, *41*, 537–546; e) I.-R. Jeon, R. Clérac, *Dalton Trans.* **2012**, *41*, 9569–9586.
[6] C. J. Milios, R. E. P. Winpenny, *Struct. Bonding* **2015**, *164*, 1–110.
[7] R. Inglis, C. J. Milios, L. F. Jones, S. Piligkos, E. K. Brechin, *Chem. Commun.* **2012**, *48*, 181–190.
[8] R. Bagai, G. Christou, *Chem. Soc. Rev.* **2009**, *38*, 1011–1026.
[9] D. Gatteschi, R. Sessoli, *Angew. Chem. Int. Ed.* **2003**, *42*, 268–297; *Angew. Chem.* **2003**, *115*, 278.
[10] B. Gerey, E. Gouré, J. Fortage, J. Pécaut, M.-N. Collomb, *Coord. Chem. Rev.* **2016**, *319*, 1–24.
[11] J. Yano, V. Yachandra, *Chem. Rev.* **2014**, *114*, 4175–4205.
[12] S. Mukherjee, J. A. Stull, J. Yano, T. C. Stamatatos, K. Pringouri, T. A. Stich, K. A. Abboud, R. D. Britt, V. K. Yachandra, G. Christou, *Proc. Natl. Acad. Sci. USA* **2012**, *109*, 2257–2262.
[13] R. Sessoli, H.-L. Tsai, A. R. Schake, S. Wang, J. B. Vincent, K. Folting, D. Gatteschi, G. Christou, D. N. Hendrickson, *J. Am. Chem. Soc.* **1993**, *115*, 1804–1816.
[14] W. Wernsdorfer, N. E. Chakov, G. Christou, *Phys. Rev. Lett.* **2005**, *95*, 037203.
[15] S. T. Adams, E. H. da Silva Neto, S. Datta, J. F. Ware, C. Lampropoulos, G. Christou, Y. Myaesoedov, E. Zeldov, J. R. Friedman, *Phys. Rev. Lett.* **2013**, *110*, 087205.
[16] M. Ganzhorn, S. Klyatskaya, M. Ruben, W. Wernsdorfer, *Nat. Nanotechnol.* **2013**, *8*, 165–169.
[17] J. H. Atkinson, A. D. Fournet, L. Bhaskaran, Y. Myasoedov, E. Zeldov, E. del Barco, S. Hill, G. Christou, J. R. Friedman, *Phys. Rev. B* **2017**, *95*, 184403.
[18] A. Cornia, M. Mannini, P. Sainctavit, R. Sessoli, *Chem. Soc. Rev.* **2011**, *40*, 3076–3091.
[19] G. Rogez, B. Donnio, E. Terazzi, J.-L. Gallani, J.-P. Kappler, J.-P. Bucher, M. Drillon, *Adv. Mater.* **2009**, *21*, 4323–4333.
[20] C. Lampropoulos, G. Redler, S. Data, K. A. Abboud, S. Hill, G. Christou, *Inorg. Chem.* **2010**, *49*, 1325–1336.
[21] C. Lampropoulos, M. Murugesu, A. G. Harter, W. Wernsdorfer, S. Hill, N. S. Dalal, A. P. Reyes, P. L. Kuhns, K. A. Abboud, G. Christou, *Inorg. Chem.* **2013**, *52*, 258–272.
[22] A. D. Fournet, K. J. Mitchell, W. Wernsdorfer, K. A. Abboud, G. Christou, *Inorg. Chem.* **2017**, *56*, 10706–10716.
[23] T. A. Jenkins, M. Garnero, S. A. Corrales, E. R. Williams, A. M. Mowson, A. Ozarowski, W. Wernsdorfer, G. Christou, C. Lampropoulos, *Inorg. Chem.* **2017**, *56*, 14755–14758.
[24] a) S. A. Corrales, J. M. Cain, K. A. Uhlig, A. M. Mowson, C. Papatriantafyllopoulou, M. K. Peprah, A. Ozarowski, A. J. Tasiopoulos, G. Christou, M. W. Meisel, C. Lampropoulos, *Inorg. Chem.* **2016**, *55*, 1367–1369; b) G. Maayan, N. Gluz, G. Christou, *Nat. Catal.* **2018**, *1*, 48–54.
[25] D. Aulakh, H. Xie, Z. Shen, A. Harley, X. Zhang, A. A. Yakovenko, K. R. Dunbar, M. Wriedt, *Inorg. Chem.* **2017**, *56*, 6965–6972.

[26] A. J. Tasiopoulos, W. Wernsdorfer, K. A. Abboud, G. Christou, *Angew. Chem. Int. Ed.* **2004**, *43*, 6338–6342; *Angew. Chem.* **2004**, *116*, 6498.
[27] A. J. Tasiopoulos, W. Wernsdorfer, K. A. Abboud, G. Christou, *Inorg. Chem.* **2005**, *44*, 6324–6338.
[28] P. King, W. Wernsdorfer, K. A. Abboud, G. Christou, *Inorg. Chem.* **2005**, *44*, 8659–8669.
[29] A. J. Tasiopoulos, A. Vinslava, W. Wernsdorfer, K. A. Abboud, G. Christou, *Angew. Chem. Int. Ed.* **2004**, *43*, 2117–2121; *Angew. Chem.* **2004**, *116*, 2169.
[30] A. Vinslava, A. J. Tasiopoulos, W. Wernsdorfer, K. A. Abboud, G. Christou, *Inorg. Chem.* **2016**, *55*, 3419–3430.
[31] M. Charalambous, E. E. Moushi, C. Papatriantafyllopoulou, W. Wernsdorfer, V. Nastopoulos, G. Christou, A. J. Tasiopoulos, *Chem. Commun.* **2012**, *48*, 5410–5412.
[32] M. Manoli, S. Alexandrou, L. Pham, G. Lorusso, W. Wernsdorfer, M. Evangelisti, G. Christou, A. J. Tasiopoulos, *Angew. Chem. Int. Ed.* **2016**, *55*, 679–684; *Angew. Chem.* **2016**, *128*, 689.
[33] M. Manoli, R. Inglis, S. Piligkos, L. Yanhua, W. Wernsdorfer, E. K. Brechin, A. J. Tasiopoulos, *Chem. Commun.* **2016**, *52*, 12829–12832.
[34] P. Abbasi, K. Quinn, D. I. Alexandropoulos, M. Damjanović, W. Wernsdorfer, A. Escuer, J. Mayans, M. Pilkington, T. C. Stamatatos, *J. Am. Chem. Soc.* **2017**, *139*, 15644–15647.
[35] a) D. I. Alexandropoulos, A. Fournet, L. Cunha-Silva, G. Christou, T. C. Stamatatos, *Inorg. Chem.* **2016**, *55*, 12118–12121; b) Y.-K. Deng, H.-F. Su, J.-H. Xu, W.-G. Wang, M. Kurmoo, S.-C. Lin, Y.-Z. Tan, J. Jia, D. Sun, L.-S. Zheng, *J. Am. Chem. Soc.* **2016**, *138*, 1328–1334; c) L.-Y. Guo, H.-F. Su, M. Kurmoo, C.-H. Tung, D. Sun, L.-S. Zheng, *J. Am. Chem. Soc.* **2017**, *139*, 14033–14036; F. Yang, Y.-K. Deng, L.-Y. Guo, H.-F. Su, Z. Jagličić, Z.-Y. Feng, G.-L. Zhuang, S.-Y. Zeng, D. Sun, *CrystEngComm* **2016**, *18*, 1329–1336.
[36] E. E. Moushi, A. Masello, W. Wernsdorfer, V. Nastopoulos, G. Christou, A. J. Tasiopoulos, *Dalton Trans.* **2010**, *39*, 4978–4985.
[37] E. E. Moushi, T. C. Stamatatos, W. Wernsdorfer, V. Nastopoulos, G. Christou, A. J. Tasiopoulos, *Angew. Chem. Int. Ed.* **2006**, *45*, 7722–7725; *Angew. Chem.* **2006**, *118*, 7886.
[38] E. E. Moushi, C. Lampropoulos, W. Wernsdorfer, V. Nastopoulos, G. Christou, A. J. Tasiopoulos, *J. Am. Chem. Soc.* **2010**, *132*, 16146–16155.
[39] I. D. Brown, D. Altermatt, *Acta Crystallogr., Sect. B* **1985**, *41*, 244–247.
[40] W. Liu, H. H. Thorp, *Inorg. Chem.* **1993**, *32*, 4102–4105.
[41] a) D. J. Price, S. R. Batten, B. Moubaraki, K. S. Murray, *Chem. Commun.* **2002**, 762–763; b) P. King, W. Wernsdorfer, K. A. Abboud, G. Christou, *Inorg. Chem.* **2004**, *43*, 7315–7323.
[42] J. T. Brockman, J. C. Huffman, G. Christou, *Angew. Chem. Int. Ed.* **2002**, *41*, 2506–2508; *Angew. Chem.* **2002**, *114*, 2616.
[43] a) J. B. Vincent, H.-R. Chang, K. Folting, J. C. Huffman, G. Christou, D. N. Hendrickson, *J. Am. Chem. Soc.* **1987**, *109*, 5703–5711; b) J. B. Vincent, C. Christmas, H.-R. Chang, Q. Li, P. D. W. Boyd, J. C. Huffman, D. N. Hendrickson, G. Christou, *J. Am. Chem. Soc.* **1989**, *111*, 2086–2097.
[44] Oxford Diffraction. *CrysAlis CCD and CrysAlis RED*; Oxford Diffraction Ltd.: Abingdon, UK, **2008**.
[45] M. C. Burla, R. Caliandro, M. Camalli, B. Carrozzini, G. L. Cascarano, L. De Caro, C. Giacovazzo, G. Polidori, R. Spagna, *J. Appl. Crystallogr.* **2005**, *38*, 381–388.
[46] Sheldrick, G. M. *SHELXL-**2014**/7*, Program for Refinement of Crystal Structures; University of Göttingen: Germany, **2014**.
[47] L. J. Farrugia, *J. Appl. Crystallogr.* **1999**, *32*, 837–838.
[48] K. Brandenburg, "*Diamond, Version 3.1d. Crystal impact GbR*", Bonn, Germany, **2006**.
[49] a) A. L. Spek, *PLATON, A multipurpose crystallographic tool*; Utrecht University: Utrecht, The Netherlands, **2003**; b) P. van der Sluis, A. L. Spek, *Acta Crystallogr., Sect. A* **1990**, *46*, 194.

Received: June 16, 2018

